# **Analytical Equations for Predicting Effective Thermal Conductivity in Laminated Wood Composites**

Harsh Pal a and Sardar Malek , b,\*

This paper presents an analytical modeling approach to predict the effective in-plane and out-of-plane thermal conductivities of laminated wood composite products such as Cross-Laminated Timber (CLT). Considering wood's orthotropic nature, having models that could be used to estimate the effective thermal conductivity properties of laminated wood products in various directions becomes essential for understanding the coupling between mechanical and thermal properties, as well as predicting the dimensional stability of large wood composite panels. For this purpose, analytical thermal conductivity equations were derived in three orthogonal directions, considering different properties of wood along its orthotropic directions, following Fourier's Law. The derived equations were then applied to different CLT panel products and results were compared to assess their accuracy. As CLT panels may be produced without edge gluing, two scenarios were investigated to understand the effect of edge gluing on thermal conductivity of such panels. First, the presence of adhesive between timber layers was ignored (i.e. not edge-glued panels); second, adhesive and its thickness were included. Results demonstrated the reasonable accuracy of the proposed approach in predicting the thermal conductivity of CLT panels made with different gluing methods. The modeling of imperfect bonds and air gaps is also briefly discussed.

DOI: 10.15376/biores.20.1.2150-2170

Keywords: Thermal conductivity; Timber; Adhesives; Cross-Laminated Timber (CLT); Heat transfer model; Modeling; Orthotropic materials

Contact information: a: Department of Mechanical and Industrial Engineering, Indian Institute of Technology, Roorkee, Uttarakhand 247667 India; b: Department of Civil Engineering, University of Victoria, Victoria, BC V8P 5C2 Canada; \*Corresponding author: smalek@uvic.ca

## INTRODUCTION

In the past two decades, the global timber market has experienced remarkable growth, resulting in a heightened utilization of wood as a primary construction material across a range of projects including residential and commercial buildings (Saavedra *et al.* 2015). Advancements in mass timber engineering have sparked a renewed sense of purpose and expanded the versatility of wood as a building material. As environmental concerns continue to rise, the significance of wood-based structures is becoming increasingly apparent compared to traditional materials such as steel and concrete. This growing recognition is expected to drive further progress towards sustainable construction solutions and greener materials.

Wood is known for its heterogeneous and orthotropic nature, characterized by a complex structure spanning multiple length scales (Malek and Gibson 2017). To represent this complexity accurately, researchers have been developing multiscale models utilizing finite element simulations and computational homogenization techniques to analyze the

mechanical properties of wood and its composites (Malekmohammadi *et al.* 2015; Malek and Gibson 2017). In mass timber construction, a key design concept for building insulation materials is to target a low thermal conductivity (*k*-value) for laminated wall and floor panels. CLT, a mass timber laminated product, is commonly produced by bonding multiple softwood or hardwood wood layers using a small amount of adhesive, which is often ignored in analysis of such products (Afshari and Malek 2022).

Although the thermal conductivity of wood and fiber-based composites is well investigated in the literature, effective thermal conductivity of laminated wood composites is less explored in the literature. For instance, extensive research, both numerical and experimental, has been conducted to study elastic and thermomechanical properties of wood-concrete composite made with wood chips. Taoukil *et al.* (2013) explored the impact of moisture content on the thermal conductivity and diffusivity of wood-concrete composites. Additionally, Akkaoui *et al.* (2017) explored modelling such composites and comparing testing data with analytical homogenization and modelling predictions based on classical micromechanics schemes such as Mori-Tanaka or self-consistent models assuming spherical or ellipsoidal inclusions.

It should be noted that although classical micromechanical may be used for composite with low to moderate volume fractions of fibers ( $V_f < 75\%$ ), such approaches are not applicable to highly-filled composites with orthotropic fibers, such as strand-based wood composites and CLT, due to the key assumptions made in their development (see Malekmohammadi *et al.* (2015) and Malek *et al.* (2019)). Despite extensive research on wood composite materials, specific models for predicting the orthotropic thermal conductivity of laminated wood composites such as CLT, Laminated Veneer Lumber (LVL), and Parallel Strand Lumber (PSL) are still missing. Existing models are either too simplistic (ignoring the presence of adhesives or mismatching properties in different directions) or overly complex (*e.g.*, requiring detailed 3D numerical finite element models (Afshari and Malek 2022)). Simple models typically assume that wood is an isotropic material and fail to account for the unique layered structure and bonding characteristics of CLT. This gap in the literature highlights the need for a relatively simple but also an accurate approach that can be implemented by panel producers to optimize the performance of their products.

To address the above research gap, a general analytical modeling approach is presented to study the thermal behavior of laminated wood composites. Some key assumptions are made in deriving analytical equations to estimate the effective thermal conductivities of such composites in 3 orthogonal directions: First, conduction is assumed to be the main mechanism of heat transfer. Second, moisture content is assumed to be constant within the entire panel. Third, resin diffusion into the wood pores is ignored. Unlike previous studies, the resin layer is idealized as a perfect adhesive layer with constant layer thickness bonding the wood surfaces. In other words, the resin is treated as a continuous, thin isotropic situated between thicker orthotropic wood layers. Furthermore, it is assumed that all wood planks have identical properties (e.g., density and moisture content). It should be noted that although these assumptions seem very basic and ideal, they could be released, and applicability of the model be extended. To model the air gaps that may occur in real panels, the interface may be idealized as voids with negligible thermal conductivity representing air's thermal conductivity.

Through physics-based analytical modeling as presented in the paper and validated against experimental measurements, researchers could understand the importance of various design parameters such as the thickness or thermal conductivity of resin compared

to wood properties and hence optimize the design and efficacy of wood-based composites, fostering sustainability and efficiency across a spectrum of engineering applications. As research on green wood composites progresses, continued exploration of thermomechanical properties, in addition to mechanical properties, will yield further insights into their performance under extreme environmental conditions (Chiniforush *et al.* 2022), advancing sustainable materials and green construction methodologies.

The paper is structured into four main sections. In the modeling approach section, the theoretical foundations of thermal conductivity are described, followed by the development of specific mathematical equations for calculating thermal conductivity. The comparison of these equations with the Halpin-Tsai model is explored, and suggestions are made to tailor them for CLT panels in the results section. Subsequently, the validity of the formulated equations is confirmed through their comparison with experimental results.

## MODELING APPROACH

In 1822, Fourier introduced the theory of thermal conductivity, which states that heat flow within a homogeneous medium is directly proportional to the negative temperature gradient. This principle forms the basis of one-dimensional (1-D) steady-state heat transfer analysis, where heat flow is typically assumed to occur exclusively in the x-direction. Mathematically, this theory can be expressed as:

$$q_x = -k_x A \frac{dT}{dx} \tag{1}$$

where  $q_x$  denotes the steady-state heat flux crossing the assumed differential boundary, and  $k_x$  represents the material thermal conductivity. In the above equation, A is the cross-sectional area and  $\frac{dT}{dx}$  is the temperature gradient in the x-direction (see Fig. 1). Rearranging the terms in Eq. 1, the thermal conductivity in the x-direction can be written as:

$$k_{x} = -\frac{q_{x}}{A} \frac{\Delta L}{\Delta T} \tag{2}$$

It should be noted that  $k_x$  is the thermal conductivity in W/mK,  $q_x$  is the heat flux in W/m<sup>2</sup>, and  $\Delta T$  is the temperature difference in K.  $\Delta L$  is the distance in m. Hence, the thermal conductivity of a material can be defined as the measure of its efficiency in conducting heat across a specific unit area when subjected to a temperature gradient along its cross-sectional area (A).

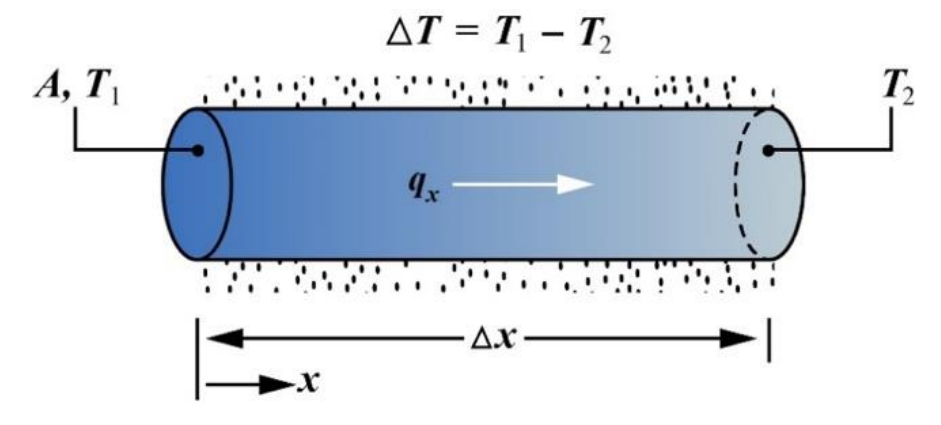


Fig. 1. Schematic of steady state heat conduction in 1-D according to Fourier's law

# **Effective Thermal Conductivity in 1-D**

In 1-D heat transfer under the assumption of no internal energy generation and constant material properties, a parameter can be defined called the material's thermal resistance  $(R_t)$ . This parameter signifies the material's resistance to the flow of heat across its cross-section and can be expressed as:

$$R_t = \frac{\Delta T}{q_x} \tag{3}$$

For materials composed of multiple layers, such as two-layered materials (or multi-layered configurations in general), the heat flow through distinct materials can be represented using thermal circuits (refer to Fig. 2 for heat flow through a two-layered material). For this purpose, Eq. 2 can be rearranged and written as:

$$\frac{\Delta T}{q_x} = \frac{L}{k_x A} \tag{4}$$

hence.

$$R_t = -\frac{T_1 - T_2}{q_x} = \frac{L}{k_x A} \tag{5}$$

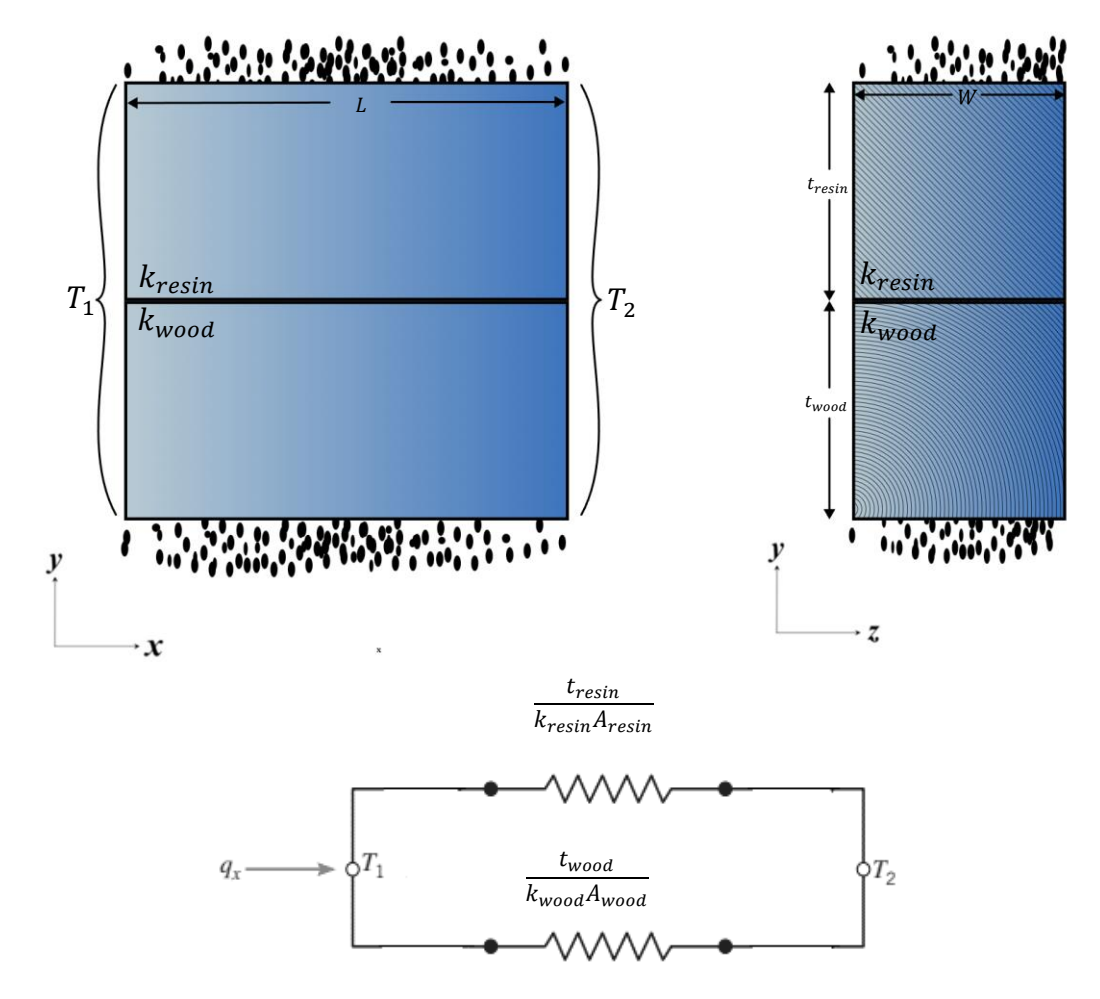


**Fig. 2.** Heat flow through a two-layered material, consisting of wood and resin, represented using thermal circuits. Front and side views are shown in top left and right, respectively

In Fig. 2, L and W denote the length and width of the wood and resin layer, respectively. Therefore, the cross-sectional area available for heat conduction from the

outside through the resin layer becomes  $W \times t_{\rm resin}$ , and the cross-sectional area available for heat conduction through the wood becomes  $W \times t_{\rm wood}$  (where t represents the material thickness). The total heat flowing through this orientation will be the sum of heat passing through the resin layer  $(q_{\rm resin})$  and the wood  $(q_{\rm wood})$ , respectively:

$$q_x = q_{\text{wood}} + q_{\text{resin}} \tag{6}$$

Applying Fourier law, one can write:

$$q_{
m wood} = -k_{
m wood} (Wt_{
m wood}) \frac{T_2 - T_1}{L}$$
 and,  
 $q_{
m resin} = -k_{
m resin} (Wt_{
m resin}) \frac{T_2 - T_1}{L}$ 

Hence,

$$q_{x} = -(k_{\text{resin}}Wt_{\text{resin}} + k_{\text{wood}}Wt_{\text{wood}})(\frac{T_{2} - T_{1}}{L}) = -k_{\text{eff,x}}(Wt_{\text{resin}} + Wt_{\text{wood}})\frac{T_{2} - T_{1}}{L}$$
(7)

where  $k_{\rm eff,x}$  represent the effective thermal conductivity of the layered composite system along its longitudinal direction. Simplifying the above and rearranging for  $k_{\rm eff,x}$ , this leads to:

$$k_{\text{eff,x}} = \frac{k_{\text{resin}} \cdot t_{\text{resin}} + k_{\text{wood}} \cdot t_{\text{wood}}}{t_{\text{resin}} + t_{\text{wood}}}$$
(8)

The same equation can be derived using thermal resistance (Eq. 5). Assuming similar temperature difference across the wood and resin layer, Eq. 6 can be expressed as:

$$\frac{T_1 - T_2}{R_{\text{eff}}} = \frac{T_1 - T_2}{R_{\text{resin}}} + \frac{T_1 - T_2}{R_{\text{wood}}} \tag{9}$$

$$\frac{1}{R_{\text{eff}}} = \frac{1}{R_{\text{resin}}} + \frac{1}{R_{\text{wood}}} \tag{10}$$

This may be referred to as the parallel model for simplicity.

$$\frac{k_{\text{eff,x}}(A_{\text{wood}} + A_{\text{resin}})}{I_{L}} = \frac{k_{\text{resin}}A_{\text{resin}}}{I_{L}} + \frac{k_{\text{wood}}A_{\text{wood}}}{I_{L}} \tag{11}$$

$$k_{\text{eff,x}} = \frac{k_{\text{resin}} \cdot t_{\text{resin}} + k_{\text{wood}} \cdot t_{\text{wood}}}{t_{\text{resin}} + t_{\text{wood}}}$$
(12)

Note that  $A_{resin}$  is  $Wt_{resin}$ , and  $A_{wood}$  is  $Wt_{wood}$ .

Equation 12 is similar to Eq. 8, indicating that the thermal resistance analogy accurately estimates the effective thermal conductivity. It is also demonstrable that the thermal conductivity along the longitudinal (x-) direction can be approximated using the equation derived from the rule of mixtures. This equation is formulated based on the assumption that, when a heat flux is applied along the fiber (reinforcement) direction of a composite system, the composite constituents (i.e., fiber and matrix) can be substituted with an equivalent system of homogeneous blocks. These blocks have volumes proportional to their relative volume in the composite. Analogous to the thermal resistance and employing a mechanical analogy, the thermal conductivity of a two-layered material in the longitudinal direction can be estimated as follows,

$$k_{\text{eff,x}} = V_f k_f + (1 - V_f) k_{\text{resin}} \tag{13}$$

where  $V_f$  is the fiber volume fraction and  $k_f$  and  $k_{resin}$  are the thermal conductivities of fiber (here wood) and resin, respectively. Knowing the wood and resin volume to be  $L \times W \times t_{wood}$  and  $L \times W \times t_{resin}$ , respectively,  $V_f$  becomes:

$$V_f = \frac{LWt_{\text{wood}}}{LWt_{\text{resin}} + LWt_{\text{wood}}} = \frac{t_{\text{wood}}}{t_{\text{resin}} + t_{\text{wood}}}$$
(14)

Substituting  $V_f$  from the above equation in Eq. 13:

$$k_{\text{eff,x}} = \frac{k_{\text{resin}} \cdot t_{\text{resin}} + k_{\text{wood}} \cdot t_{\text{wood}}}{t_{\text{resin}} + t_{\text{wood}}}$$
(15)

The above equation is identical to Eq. 8, which was derived using Fourier's Law. Therefore, reducing the model to an analogous parallel model and employing the rule of mixture equation yield the same equations for estimating the effective thermal conductivity of a two-layered composite material in the longitudinal direction of fibers (here, wood grain).

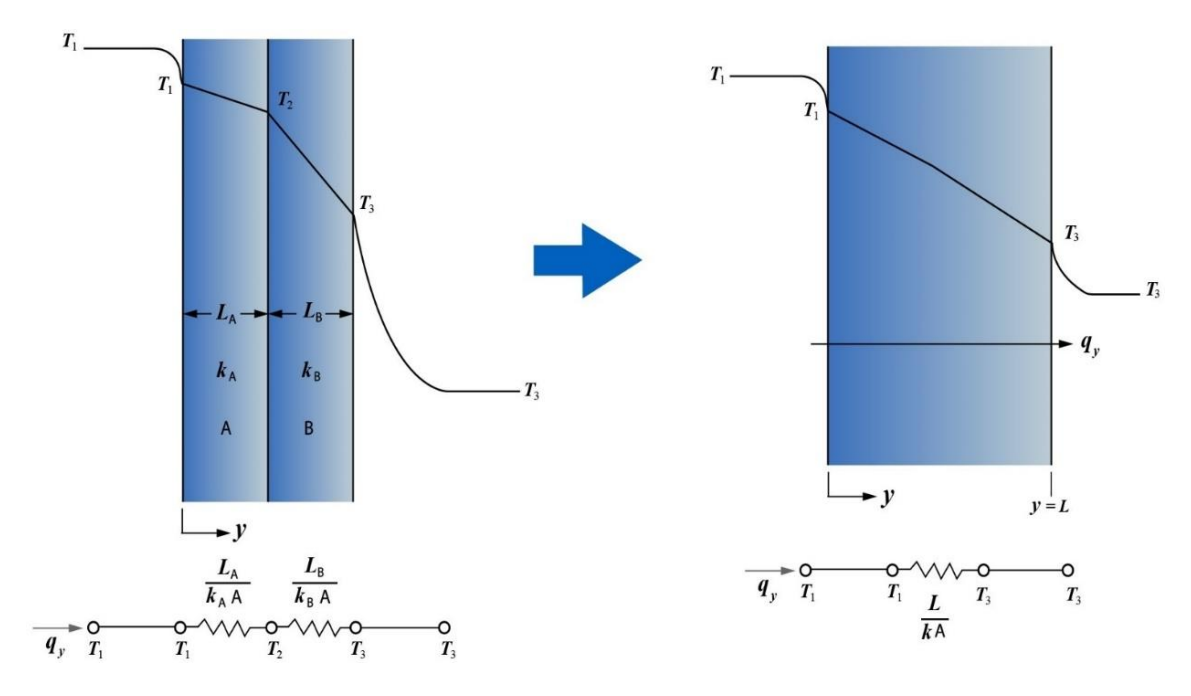


Fig. 3. Equivalent thermal circuit for the transverse direction of the two-layer wood composite

In the transverse y-direction, as shown in Fig. 3, it is possible to derive the expression for  $k_{\rm eff}$  using Fourier law's equations, similar to the way in which it was derived for the longitudinal direction. Because there is temperature gradient across the material, Fourier's Law at surface A and B can be written as:

$$q_y = -k_A \left(\frac{T_2 - T_1}{L_A}\right) = -k_B \left(\frac{T_3 - T_2}{L_B}\right) = -k_{\text{eff,y}} \left(\frac{T_3 - T_1}{L_B + L_A}\right)$$
 (16)

Solving for  $T_2$ :

$$T_2 = \frac{k_B L_A T_3 + k_A L_B T_1}{k_A L_B + k_B L_A} \tag{17}$$

Considering the second part of the Eq. 16 and substituting the value of  $T_2$ :

$$k_{\text{eff,y}} = \frac{k_A k_B (L_A + L_B)}{k_A L_B + k_B L_A} \tag{18}$$

After rearranging, this leads to:

$$\frac{1}{k_{\text{eff,y}}} = \frac{1}{L_B + L_A} \left( \frac{L_A}{k_A} + \frac{L_B}{k_B} \right) \tag{19}$$

Assuming that the surface A and B in Fig. 3 represent the cross-sectional area of resin and wood with thicknesses  $t_r$  and  $t_w$ , and with thermal conductivities of  $k_r$  and  $k_w$ , respectively, then  $k_{\text{eff,v}}$  will be:

$$k_{\text{eff,y}} = \frac{k_r k_w (t_r + t_w)}{k_r t_w + k_w t_r} \tag{20}$$

Now, deriving the same equation using the thermal resistance as defined in Eq. 5,  $R_{\text{eff}} = R_{\text{resin}} + R_{\text{wood}}$  with:

$$\frac{t_{\text{wood}} + t_{\text{resin}}}{k_{\text{eff,y}}A} = \frac{t_{\text{resin}}}{k_{\text{resin}}A} + \frac{t_{\text{wood}}}{k_{\text{wood}}A}$$
(21)

Through factoring, the above can be rearranged for  $k_{\text{eff,v}}$  and written as:

$$\frac{1}{k_{\text{eff,v}}} = \frac{1}{t_{\text{wood}} + t_{\text{resin}}} \left( \frac{t_{\text{resin}}}{k_{\text{resin}}} + \frac{t_{\text{wood}}}{k_{\text{wood}}} \right) \tag{22}$$

It can be shown that Eq. 22 is the same as Eq. 20 using Fourier Law, demonstrating that the thermal resistance analogy can be applied in the transverse direction.

# Halpin-Tsai Model

The Halpin-Tsai model (Ashton *et al.* (1969)) consists of a set of mathematical equations originally proposed to predict the elastic moduli of short-fiber composite materials. The model considers the geometry and orientation of the reinforcing constituents (fibers, particles) within a matrix, as well as the elastic properties of both the reinforcement and the surrounding matrix.

In the Halpin and Tsai approach which is based on Hill's self-consistent model for predicting the elastic moduli, mechanical stresses and strains are represented by their averaged values in individual constituents. By drawing an analogy between thermal stress and mechanical stress in the composite constituents under thermal loading, the same form of equations could be used to estimate the effective thermal conductivity of the composite  $(k_c)$ , analogous to effective elastic moduli of the composite  $(E_c)$ , in a specific direction as follows:

$$k_c = k_{\text{resin}} \left( \frac{1 + \zeta \eta V_f}{1 - \eta V_f} \right) \tag{23}$$

$$\eta = \frac{\frac{k_f}{k_{\text{resin}} - 1}}{\frac{k_f}{k_{\text{resin}}} + \zeta} \tag{24}$$

where  $\zeta$  is the empirical geometric shape parameter used to accommodate the discontinuous arrangement of fibers in a general short fiber composite. Halpin and Tsai used their approach to analytically derive a solution, with the inclusion of the experimental shape parameter  $\zeta$  to account for different shapes of reinforcements (fibers).

For a better understanding of the parameter  $\zeta$ , its effect on the Halpin-Tsai equations is shown below. Note that the extreme (upper and lower bound) cases for  $\zeta$  are  $\zeta=0$  and  $\zeta=\infty$ .

a) For  $\zeta \to \infty$ ,

$$\lim_{\zeta \to \infty} \frac{k_c}{k_{resn}} = \lim_{\zeta \to \infty} \left( \frac{-(k_f + \zeta k_{resin} + \zeta V_f k_f - \zeta V_f k_{resin})}{(-k_f - \zeta k_{resin} + V_f k_f - V_f k_{resin})} \right)$$
(25)

Applying L-Hopital's rule:

$$\lim_{\zeta \to \infty} \frac{k_c}{k_{resn}} = \frac{\frac{\partial \left( -\left(k_f + \zeta k_{\text{resin}} + \zeta V_f k_f - \zeta V_f k_{\text{resin}}\right)\right)}{\partial \zeta}}{\frac{\partial \left( -k_f - \zeta k_{\text{resin}} + V_f k_f - V_f k_{\text{resin}}\right)}{\partial \zeta}}$$
(26)

Leads to:

$$k_c = v_f k_f + (1 - V_f) k_{\text{resin}}$$
 {Same as Eq. 13}

Thus, for  $\zeta \to \infty$  the Halpin-Tsai equation reduces to the longitudinal equation Eq. 15.

b) Similarly, for  $\zeta = 0$ ,

$$k_c = k_{resin} \left( \frac{1}{1 - \eta V_f} \right) = \frac{1}{\left( \frac{V_f}{k_f} + \frac{1 - V_f}{k_{resin}} \right)}$$
(27)

Or,  $\frac{1}{k_c} = \left(\frac{V_f}{k_f} + \frac{1 - V_f}{k_{\rm resin}}\right)$  which is similar to Eq.22 by substituting  $V_f = \frac{t_{\rm wood}}{t_{\rm wood} + t_{\rm resin}}$ . Thus, for  $\zeta = 0$ , the Halpin-Tsai equation reduces to the transverse model we obtained here. This demonstrates that the analogy for Halpin and Tsai equations could lead to similar equations for estimating the effective thermal conductivity of wood composites.

## Comparison with Halpin-Tsai Model

The comparison of the derived equations with the Halpin-Tsai equations reveals a close match for estimating the thermal conductivity of composites. Inspecting the role of the shape parameter  $\zeta$  shows that the derived equations effectively capture the influence of fiber geometry and distribution within the composite material. When  $\zeta \rightarrow \infty$ , the Halpin-Tsai is reduced to the longitudinal thermal conductivity model obtained in this paper. On the other hand, when  $\zeta$ =0, the Halpin-Tsai equation is reduced to the transverse thermal conductivity model.

## **Effective Thermal Conductivity in 3-D**

Using the same approach and above equations (Eqs. 8 and 22), it is possible to generalize the effective thermal conductivity in three dimensions as,

$$k_{\chi\chi} = \frac{k_{\text{resin}} \cdot t_{\text{resin}} + k_{\text{wood}-l} \cdot t_{\text{wood}}}{t_{\text{resin}} + t_{\text{wood}}}$$

$$k_{\chi\chi} = \frac{k_{\text{resin}} k_{\text{wood}-t} (t_{\text{resin}} + t_{\text{wood}})}{k_{\text{resin}} t_{\text{wood}} + k_{\text{wood}-t} t_{\text{resin}}}$$
(29)

$$k_{yy} = \frac{k_{\text{resin}}k_{\text{wood}-t}(t_{\text{resin}}+t_{\text{wood}})}{k_{\text{resin}}t_{\text{wood}}+k_{\text{wood}-t}t_{\text{resin}}}$$
(29)

$$k_{zz} = \frac{k_{\text{resin}} \cdot t_{\text{resin}} + k_{\text{wood}} - r \cdot t_{\text{wood}}}{t_{\text{resin}} + t_{\text{wood}}}$$
(30)

where  $k_{\text{wood}-l}$ ,  $k_{\text{wood}-r}$ ,  $k_{\text{wood}-t}$  are the thermal conductivities of wood along its longitudinal (*l*), radial (*r*), and tangential (*t*) directions, respectively.

Applying Fourier's Law, the above equations can be expressed in tensorial notation,

$$q = -k\nabla T \tag{31}$$

where q is the conduction heat flux vector and k is the thermal conductivity tensor with  $k_{xx}, k_{yy}$ , and  $k_{zz}$  components. Given the continuous nature of the matrix in the composite, it is logical to consider both the fiber and matrix as constituents of a composite unit cell. In this context, the unit cell is defined as the smallest repeating unit of the microstructure in the composite (specifically, wood and resin in this study) consisting of its two main constituents: the fiber and matrix. Consequently, the effective conductivity of the unit cell is linked to the macroscopic flux and temperature gradients within the composite laminate. These macroscopic parameters are characterized as surface averages of their corresponding microscopic counterparts, as outlined in Temizer and Wriggers et al. (2010). Hence, they can be expressed as follows,

$$\bar{q} = \langle q \rangle = \frac{1}{S} \int_{S} q. \, dS \tag{32}$$

$$\overline{\nabla T} = \langle \nabla T \rangle = \frac{1}{c} \int_{c} \nabla T \, dS \tag{33}$$

where  $\langle . \rangle$  denotes the average quantity, S is the surface of integration, q is the microscopic heat flux, and  $\nabla T$  is the microscopic thermal gradient. It can be seen that the effective thermal conductivity is related to the surface averaged thermal quantities as

$$\overline{k_{\rm eff}} = -\frac{\overline{q}}{\overline{VT}} \tag{34}$$

where  $k_{\rm eff}$  is the effective thermal conductivity vector.

Utilizing Eq. 32 and Eq. 33, Eq. 34 can be expressed in three dimensions as follows:

$$\frac{1}{S} \begin{bmatrix} \int_{S} q_{x} \cdot dS \\ \int_{S} q_{y} \cdot dS \\ \int_{S} q_{z} \cdot dS \end{bmatrix} = -\frac{1}{S} \begin{bmatrix} k_{xx} & 0 & 0 \\ 0 & k_{yy} & 0 \\ 0 & 0 & k_{zz} \end{bmatrix} \begin{bmatrix} \int_{S} \frac{\partial T}{\partial x} \cdot dS \\ \int_{S} \frac{\partial T}{\partial y} \cdot dS \\ \int_{S} \frac{\partial T}{\partial z} \cdot dS \end{bmatrix}$$
(35)

where S is the surface of integration,  $k_{xx}$ ,  $k_{yy}$  and  $k_{zz}$  are conductivities of the elements in the x, y and z directions respectively, and  $q_x$ ,  $q_y$  and  $q_z$  denote the heat fluxes in the x, y and z directions respectively. Hence, the effective thermal conductivity tensor can be written as:

$$\overline{k_{\text{eff}}} = -\frac{\int_{S} q.dS}{\int_{c} (n.\nabla T).dS}$$
 (36)

where n denotes the normal vector to each element boundary of the unit cell.

# **Generalization of 3-D Equations for Multiple Layers**

The above analysis for a two-layered material can be generalized to n-layered materials. Assuming an n-layer wood composite with wood layer thicknesses of  $t_{w1}, t_{w2}, t_{w3}, \dots, t_{wn}$  and n-1 layers of resin with thicknesses  $t_{r1}, t_{r2}, t_{r3}, \dots, t_{r(n-1)}$  between the wood layers, Eq. 8 can be generalized as:

$$k_{\chi\chi} = \frac{k_{\text{resin.}}(t_{r_1} + t_{r_2} + \dots + t_{r(n-1)}) + k_{\text{wood}(l)}(t_{w_1} + t_{w_2} + \dots + t_{w_n})}{(t_{w_1} + t_{w_2} + \dots + t_{w_n}) + (t_{r_1} + t_{r_2} + \dots + t_{r(n-1)})}$$
(37)

Also, in the transverse direction, Eq. 22 can be generalized as:

$$\frac{1}{k_{yy}} = \frac{1}{(t_{w1} + t_{w2} + \dots + t_{wn}) + (t_{r1} + t_{r2} + \dots + t_{r(n-1)})} \left( \frac{t_{r1} + t_{r2} + \dots + t_{r(n-1)}}{k_{resin}} + \frac{t_{w1} + t_{w2} + \dots + t_{wn}}{k_{wood(r)}} \right)$$
(38)

Similarly, from Eq. 8, it is possible to derive:

$$k_{zz} = \frac{k_{\text{resin.}}(t_{r1} + t_{r2} + \dots + t_{r(n-1)}) + k_{\text{wood}(t)}(t_{w1} + t_{w2} + \dots + t_{wn})}{(t_{w1} + t_{w2} + \dots + t_{wn}) + (t_{r1} + t_{r2} + \dots + t_{r(n-1)})}$$
(39)

## **RESULTS**

The derived equations (Eqs. 37, 38, and 39) offer a framework for establishing a system of equations to calculate the effective orthotropic thermal conductivity of CLT panels, taking based on the layup configuration (*i.e.* layer thicknesses) and thermal conductivity of wood and resin layers. To understand the role of adhesives and demonstrate the capability of the approach in capturing the role of each constituent, first it is assumed that there is no adhesive between the wood layers within each layer (*i.e.* no edge-gluing within the plane). In other words, the wood planks in each layer are perfectly contacting the neighboring wood planks. The resulting equations under this assumption are presented as Case 1 in this paper. Then, in Case 2, we consider the presence of adhesive layer within each CLT layer that was initially disregarded, to estimate the effective thermal conductivity of edge-glued panels.

# Case 1 - CLT panels without edge-gluing

Consider a 3-ply CLT panel as the simplest example of a CLT product, with wood thicknesses donated by  $t_{w1}$ ,  $t_{w2}$ , and  $t_{w3}$  and resin thicknesses, through the panel thickness, denoted by  $t_{r1}$  and  $t_{r2}$  along the panel's x-direction (see Fig. 4). Assuming the thermal conductivity of wood along its longitudinal, radial and tangential directions be denoted by  $k_{wood(l)}$ ,  $k_{wood(r)}$ ,  $k_{wood(t)}$ , respectively, the orthotropic nature of wood is considered in those derivations. It should be noted that the resin's thermal conductivity  $k_{resin}$  may represent either pure resin or resin with voids (imperfect glue lines) characteristics. If the variation of resin thermal conductivity with moisture content has been experimentally determined, this can also be incorporated into the model by modifying the properties accordingly (i.e.  $k_{modified,resin}$ ). This modified thermal conductivity of the resin, as measured, could replace  $k_{resin}$  in the equations as similar to the modified elastic modulus of resin in Malek  $et\ al.\ (2019)$ . Then, the effective thermal conductivities of the composite in all three directions can be expressed in terms of the geometry parameters and thermal conductivity values of the constituents as follows:

$$\frac{1}{k_{xx}} = \frac{1}{(t_{w1} + t_{w2} + t_{w3}) + (t_{r1} + t_{r2})} \left( \frac{t_{r1} + t_{r2}}{k_{resin}} + \frac{t_{w1} + t_{w3}}{k_{wood(r)}} + \frac{t_{w2}}{k_{wood(t)}} \right)$$
(40)

$$k_{yy} = \frac{k_{\text{resin.}}(t_{r_1} + t_{r_2}) + k_{\text{wood}(l)}(t_{w_1} + t_{w_3}) + k_{\text{wood}(t)} \cdot t_{w_2}}{(t_{w_1} + t_{w_2} + t_{w_3}) + (t_{r_1} + t_{r_2})}$$
(41)

$$k_{zz} = \frac{k_{\text{resin.}}(t_{r_1} + t_{r_2}) + k_{\text{wood}(t).}(t_{w_1} + t_{w_3}) + k_{\text{wood}(l).}t_{w_2}}{(t_{w_1} + t_{w_2} + t_{w_3}) + (t_{r_1} + t_{r_2})}$$
(42)

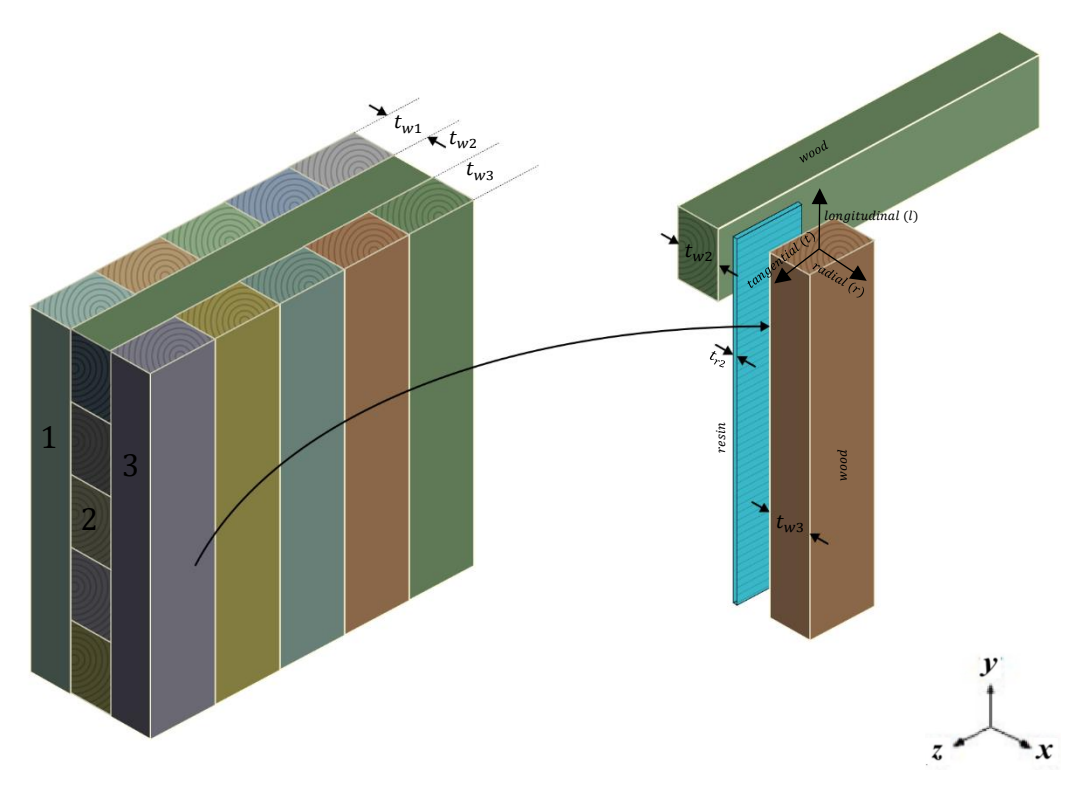


Fig. 4. CLT panel with 3-layers. The three orthotropic directions (I, r, and t) of wood are highlighted with respect to panel directions. The CLT panel is not edge-glued.

# Case 2 - CLT panels with edge-gluing

Let the width of resin between the wood planks be denoted as w' (see Fig. 5), and the thermal conductivity of the resin as  $k_{resin}$ . The other terms remain the same as in Case 1.

Now, in *x*-direction:

$$k_{1,\text{eff(x)}} = \frac{5k_{\text{wood}(r)}.w + 4k_{\text{resin}}.w'}{5w + 4w'}$$

$$k_{2,\text{eff(x)}} = \frac{5k_{\text{wood}(t)}.w + 4k_{\text{resin}}.w'}{5w + 4w'}$$

$$k_{3,\text{eff(x)}} = \frac{5k_{\text{wood}(r)}.w + 4k_{\text{resin}}.w'}{5w + 4w'}$$
(43)
$$(44)$$

$$k_{2,\text{eff(x)}} = \frac{5k_{\text{wood(t)}}.w + 4k_{\text{resin}}.w'}{5w + 4w'} \tag{44}$$

$$k_{3,\text{eff(x)}} = \frac{5k_{\text{wood}(r)}.w + 4k_{\text{resin}}.w'}{5w + 4w'}$$
(45)

hence,

$$\frac{1}{k_{xx}} = \frac{1}{3t + 2t_{resin}} \left( \frac{t}{k_{1,eff(x)}} + \frac{t}{k_{2,eff(x)}} + \frac{t}{k_{3,eff(x)}} + \frac{2t_{resin}}{k_{resin}} \right)$$
(46)

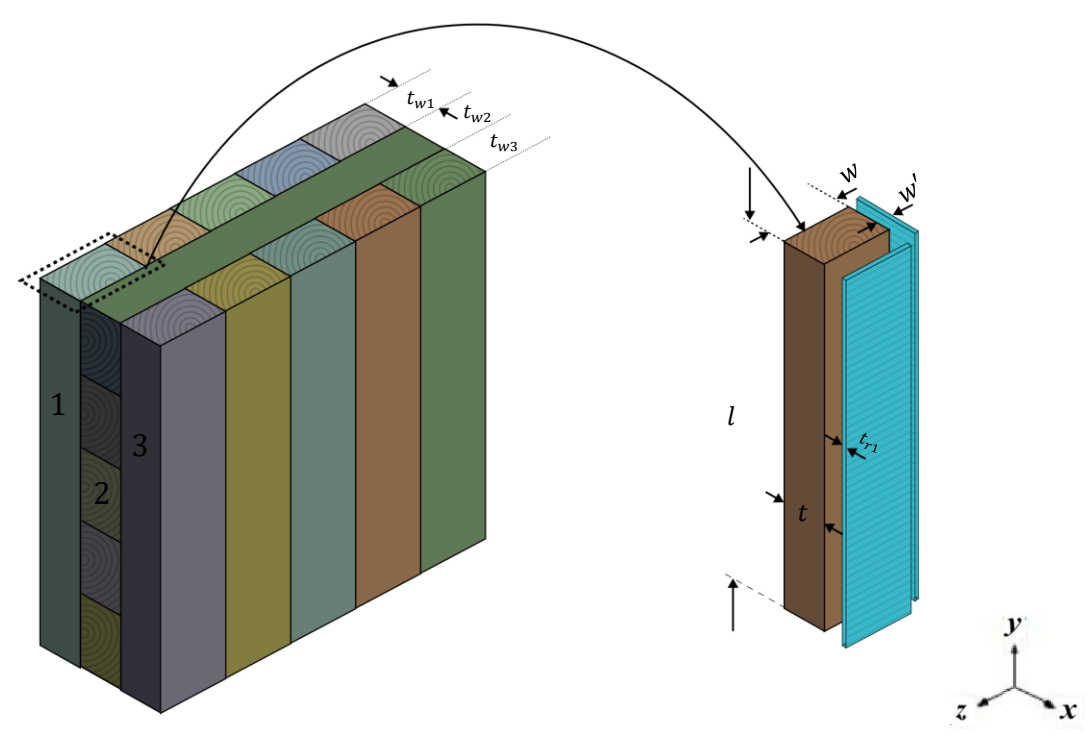


Fig. 5. Dimensions of wood planks and resin layers in a CLT panel with 3 layers. The CLT panel is edge-glued.

and in the y-direction:

$$k_{1,\text{eff}(y)} = \frac{5k_{\text{wood}(l)} \cdot w + 4k_{\text{resin}} \cdot w'}{5w + 4w'} \tag{47}$$

$$k_{1,\text{eff(y)}} = \frac{5k_{\text{wood(l)}} \cdot w + 4k_{\text{resin}} \cdot w'}{5w + 4w'}$$

$$k_{2,\text{eff(y)}} = \frac{5k_{\text{wood(r)}} \cdot w + 4k_{\text{resin}} \cdot w'}{5w + 4w'}$$
(48)

$$k_{3,\text{eff(y)}} = \frac{5k_{\text{wood(l)}} \cdot w + 4k_{\text{resin}} \cdot w'}{5w + 4w'}$$

$$(49)$$

hence,

$$k_{yy} = \frac{k_{\text{resin.}}(t_{r_1} + t_{r_2}) + t.(k_{1,\text{eff(y)}} + k_{2,\text{eff(y)}} + k_{3,\text{eff(y)}})}{3(t) + (t_{r_1} + t_{r_2})}$$
(50)

Similarly, in *z*-direction:

$$k_{1,\text{eff}(z)} = \frac{5k_{\text{wood}(t)} \cdot w + 4k_{\text{resin}} \cdot w'}{5w + 4w'}$$
(51)

$$k_{2,\text{eff(z)}} = \frac{5k_{\text{wood(l)}} \cdot w + 4k_{\text{resin}} \cdot w'}{5w + 4w'}$$
(52)

$$k_{3,\text{eff(z)}} = \frac{5k_{\text{wood(t)}} \cdot w + 4k_{\text{resin}} \cdot w'}{5w + 4w'}$$
 (53)

and

$$k_{zz} = \frac{k_{\text{resin}} \cdot (t_{r_1} + t_{r_2}) + t \cdot (k_{1,\text{eff}(z)} + k_{2,\text{eff}(z)} + k_{3,\text{eff}(z)})}{3t + (t_{r_1} + t_{r_2})}$$
(54)

## **Input Parameters**

The thermal conductivity of wood is the most important input parameter in the above equations. It should be noted that this parameter is affected by several factors such as its density, moisture content, grain direction, and temperature, along with structural irregularities due to checks and knots. Thermal conductivity increases as density, moisture content, and temperature of the wood increases (Griffiths and Kaye 1923; Wangaard et al. 1940; MacLean 1941; Narayanamurti and Ranganathan 1941; Kühlmann 1962). For wood with a density between 400 and 700 kg m<sup>-3</sup>, the conductivity perpendicular to the grain is between 0.10 and 0.18 Wm<sup>-1</sup> K<sup>-1</sup> (Niemz and Sonderegger 2017) and axial thermal conductivity is approximately 2 to 3 times higher (Ratcliffe 1964; Steinhagen et al. 1977). There are numerous studies on thermal conductivity of wood at different scales (Bučar and Straže et al. 2008; Sonderegger et al. 2011; Vay et al. 2013; Vay et al. 2021), to examine the thermal conductivity of wood at micro or macro-scale (Diaz et al. 2019; Eitelberger and Hofstetter 2011) or wood modification to enhance its thermal properties (Czajkowski et al. 2020). Recently, Li et al. (2018) reported reduced transverse thermal conductivity of basswood, i.e., 0.03 Wm<sup>-1</sup> K<sup>-1</sup> due to removal of hemicelluloses and lignin and subsequent freeze drying. According to Wood Handbook (2010) thermal conductivity is nearly the same in the radial and tangential directions (i.e. transverse directions). However, conductivity along the wood grain has been reported to be greater than its conductivity across the grain by a factor of 1.5 to 2.8, with an average of about 1.8. The thermal conductivities of different softwood species of pine and spruce are tabulated in Table 1 along with their specific gravities.

**Table 1.** Thermal Conductivities of Selected Softwood Species as Reported in *Wood Handbook* at MC of 12%

| Species       | Specific Gravity | Conductivity* (Wm <sup>-1</sup> K <sup>-1</sup> ) |  |  |  |  |  |
|---------------|------------------|---|--|--|--|--|--|
| Pine          |                  |   |  |  |  |  |  |
| Eastern White | 0.37             | 0.11  |  |  |  |  |  |
| Jack          | 0.45             | 0.13  |  |  |  |  |  |
| Loblolly      | 0.54             | 0.15  |  |  |  |  |  |
| Lodgepole     | 0.43             | 0.12  |  |  |  |  |  |
| Longleaf      | 0.62             | 0.17  |  |  |  |  |  |
| Pitch         | 0.53             | 0.15  |  |  |  |  |  |
| Ponderosa     | 0.42             | 0.12  |  |  |  |  |  |
| Red           | 0.46             | 0.13  |  |  |  |  |  |
| Shortleaf     | 0.54             | 0.15  |  |  |  |  |  |
| Slash         | 0.61             | 0.17  |  |  |  |  |  |
| Sugar         | 0.37             | 0.11  |  |  |  |  |  |
| Western White | 0.4              | 0.12  |  |  |  |  |  |
| Spruce        |                  |   |  |  |  |  |  |
| Black         | 0.43             | 0.12  |  |  |  |  |  |
| Engelmann     | 0.37             | 0.11  |  |  |  |  |  |
| Red           | 0.42             | 0.12  |  |  |  |  |  |
| Sitka         | 0.42             | 0.12  |  |  |  |  |  |
| White         | 0.37             | 0.11  |  |  |  |  |  |

<sup>\*</sup>Actual conductivities may vary by up to 20%

The thermal conductivities are provided at 12% moisture content. These values are calculated using Eq. 55 from *Wood Handbook* (2010),

$$k = G(B + C.MC) + A \tag{55}$$

where G is the specific gravity based on ovendry mass and volume, MC is the moisture content (%), and A, B, and C are constants. It should be emphasized that moisture content of the wood is an important parameter which affect its thermal conductivity. In this study, the moisture content of wood has been assumed to be 12%. It could be shown that this parameter (within its typical variation range of 5 to 15%) has a negligible impact on the calculation of effective thermal conductivity for CLT panels (indoor applications), compared to other parameters such as panel lay-up, board dimensions, and orthotropic conductivity values considered for wood. It should be noted that beyond G > 0.3, and at temperatures around 24 °C and MC < 25%, the A, B, and C coefficients are reported to be constant: A = 0.01864, B = 0.1941, C = 0.004064 with k expressed in Wm<sup>-1</sup> K<sup>-1</sup>.

# **Comparison with Experimental Data**

Softwood CLT - Case 1

In the experiment conducted by Öztürk *et al.* (2020), spruce (*Picea orientalis* L.) was used to determine the thermal conductivity of a 3-layered CLT panel. Each wood plank had dimensions of  $100 \text{ mm} \times 85 \text{ mm} \times 16 \text{ mm}$  and was glued together using polyurethane adhesive at a level of  $160 \text{ g/m}^2$ . No glue was applied at the edges (not edge-glued). The moisture content was assumed to be 12% in their study. Density and thermal conductivity of polyurethane resin was  $1.47 \text{ g/cm}^3$  and 0.513 W/mK respectively (Azemati *et al.* 2018). The average specific gravity of oriental spruce wood was  $0.416 \text{ g/cm}^3$  (Aytin *et al.* 2022).

Using Eq. 55, the thermal conductivity of wood in its longitudinal direction can be calculated as:

$$k_{\text{wood(l)}} = 0.416(0.1941 + 0.004064 \times 12) + 0.01864$$
  
 $k_{\text{wood(l)}} = 0.1197 \text{ W/(mK)}$ 

Assuming the conductivity along the grain was 1.8 times (on average) larger than conductivity across the grain, the radial and tangential thermal conductivities can be estimated as:

$$k_{\text{wood(t)}} = k_{\text{wood(r)}} = 0.0665 \text{ W/mK}$$

The thickness of the resin between two layers (*i.e.* within the panel thickness) was calculated using the density and resin spread level, assuming that the surface area where glue was applied to be  $100 \text{ mm} \times 85 \text{ mm} = 8500 \times 10^{-6} \text{ m}^2$ . The mass of glue on each surface becomes  $85 \times 10^{-4} \times 160 \text{ g} = 1.36 \text{ g}$ . Therefore, thickness of resin ( $t_r$ ) can be calculated:  $\frac{1.36}{100 \times 85 \times 10^{-2} \times 1.47} = 0.109 \text{ mm}.$  Therefore,  $t_{w1} = t_{w2} = t_{w3} = t_{w} = 16 \text{ mm},$   $t_{r1} = t_{r2} = t_{r} = 0.109 \text{ mm},$  and  $t_{r2} = t_{r3} = 0.513 \text{ W/mK}.$  Substituting the above values in Eqs. 40, 41 and 42, the effective thermal conductivity can be calculated:

$$k_{xx} = 0.0667 \frac{W}{m \text{ K}}$$
  $k_{yy} = 0.1038 \frac{W}{m \text{ K}}$   $k_{zz} = 0.0862 \frac{W}{m \text{ K}}$ 

As the y-direction is equivalent to longitudinal direction, the thermal conductivity value matched the experimental value of 0.1032~W/mK (Özturk *et al.* 2020) with an error of 0.58%.

Softwood CLT - Case 2

For this case, the thickness of resin between the wood planks is calculated similar to the way that the thickness of resin between CLT layers was calculated earlier. The area of wood surface where the adhesive is applied to can be calculated as  $100 \text{ mm} \times 16 \text{ mm} = 1600 \times 10^{-6} \text{ m}^2$ . Hence, the mass of adhesive on each surface will be  $16 \times 10^{-4} \times 160 \text{ g} = 0.256 \text{ g}$ . Therefore, thickness of adhesive is  $w' = \frac{0.256}{100 \times 16 \times 10^{-2} \times 1.47} = 0.1088 \text{ mm}$ .

In the experiment, a CLT panel with 4 wood layers was used. Therefore, the width of each wood plank can be calculated as  $w = \frac{85}{4} = 21.25$  mm.

Now in the *x*-direction,

$$k_{1,\text{eff(x)}} = \frac{4k_{\text{wood}(r)} \cdot w + 3k_r \cdot w'}{4w + 3w'} = 0.0682 \text{ W/mK} = k_{2,\text{eff(x)}} = k_{3,\text{eff(x)}}$$
 (56)

hence.

$$\frac{1}{k_{xx}} = 14.607$$
,  $k_{xx} = 0.0685 W/mK$  (57)

Similarly, in the y-direction:

$$k_{1,\text{eff(y)}} = 0.121, \ k_{2,\text{eff(y)}} = 0.0682 \ \text{and} \ k_{3,\text{eff(y)}} = 0.121$$
 (58)

Hence:

$$k_{yy} = 0.1053 \frac{W}{mK} \tag{59}$$

For the *z*-direction:

$$k_{1,\text{eff}(z)} = 0.0682, k_{2,\text{eff}(z)} = 0.121 \text{ and } k_{3,\text{eff}(z)} = 0.0682$$
 (60)

And,

$$k_{zz} = 0.0877 \frac{W}{m \, K} \tag{61}$$

The predicted value of 0.1053 for the y-direction shows a difference of 2.03% compared to the experimental value, i.e.,  $k_{\rm eff} = 0.1032 \frac{W}{mK}$  (Özturk et al. 2020). Comparing the results of the two cases shows that edge-gluing does not have a significant effect on the effective thermal conductivity across the panel thickness, if the wood boards are tightly placed.

## Hardwood CLT - Case 1

In the experiment conducted by Srivaro *et al.* (2021), coconut wood was used to determine the thermal conductivity of a 3-layered CLT panel. Each board had dimensions of 400 mm (width) × 20 mm (thickness) × 400 mm (length) and was glued together with melamine urea-formaldehyde adhesive at a spread rate of 250 g/m². The moisture content is assumed to be 12% in the article. The average density of the coconut wood is assumed to be 0.655 g/cm³. Density and thermal conductivity of melamine urea-formaldehyde resin is 1.22 g/cm³ (Aytin *et al.* 2022) and 0.1944 W/mK (Qiao and Mao *et al.* 2017; Claucherty and Sakaue *et al.* 2018), respectively.

Using Eq. 55, the thermal conductivity of wood in longitudinal direction can be obtained as:

$$k_{\text{wood}(l)} = 0.655(0.1941 + 0.004064 \times 12) + 0.01864$$

$$k_{\text{wood}(l)} = 0.1777 W/mK$$

Assuming the conductivity along the grain is 1.8 times (on average) larger than conductivity across the grain the radial and tangential thermal conductivity can be estimated to be:

$$k_{\text{wood}(t)} = k_{\text{wood}(r)} = 0.0987 W/mK$$

The thickness of the resin between two layers (within the plane) is calculated using the density and resin spread rate considering the surface area where adhesive is applied to be 400 mm  $\times$  400 mm =  $16 \times 10^{-2}$  m<sup>2</sup>. The mass of glue on each of the surfaces becomes  $16 \times 10^{-2} \times 250$  g = 40 g. Therefore, thickness of resin ( $t_r$ ) can be calculated:  $\frac{40}{400 \times 400 \times 10^{-2} \times 1.22} = 0.205$  mm. Therefore,  $t_{w1} = t_{w2} = t_{w3} = t_w = 20$  mm,  $t_{r1} = t_{r2} = t_r = 0.205$  mm, and  $t_{resin} = 0.1944$  W/mK. Substituting the above values in Eqs. 40, 41 and 42, the effective thermal conductivity can be calculated:

$$k_{xx} = 0.0991 \frac{W}{m K}$$
  $k_{yy} = 0.1517 \frac{W}{m K}$   $k_{zz} = 0.1255 \frac{W}{m K}$ 

According to Srivaro *et al.* (2021), the average thermal conductivity of CLT panels falls within the range of 0.153 to 0.264 W/mK and the estimates using equations (Eqs. 40, 41, and 42) is close to the range. Note that the *y*-direction is assumed to be the grain direction.

## Hardwood CLT - Case 2

For this case, the thickness of adhesive between the wood layers needs to be calculated using the same way that the thickness was calculated for the adhesive between CLT layers. The wood layers were glued together using a different adhesive, which is polyvinyl acetate with a spread level of  $100 \text{ g/m}^2$ . The density of the resin was  $1.1 \text{ g/cm}^3$  (Kol and Altun 2009), and the thermal conductivity was assumed as 0.2 W/mK (Qiao and Mao *et al.* 2017; Claucherty and Sakaue *et al.* 2018). Assuming the surface area where the adhesive was applied =  $400 \text{ mm} \times 20 \text{ mm} = 8 \times 10^{-3} \text{ m}^2$ , the mass of adhesive on each surface becomes  $8 \times 10^{-3} \times 100 \text{ g} = 0.8 \text{ g}$ . Therefore, the thickness of adhesive was approximately  $w' = \frac{0.8}{400 \times 20 \times 10^{-2} \times 1.1} = 0.09 \text{ mm}$ . In the experiment of CLT comprising 5 wood layers here, the width of each wood could be calculated as  $w = \frac{400}{5} = 80 \text{ mm}$ . Now, in the *x*-direction:

$$k_{1,\text{eff(x)}} = \frac{5k_{\text{wood}(r)} \cdot w + 4k_{\text{r}} \cdot w'}{5w + 4w'} = 0.0988 \text{ W/mK} = k_{2,\text{eff(x)}} = k_{3,\text{eff(x)}}$$
 (62)

hence,

$$\frac{1}{k_{xx}} = 10.0877 \to k_{xx} = 0.0992 \, W/mK \tag{63}$$

Similarly, in the y-direction:

$$k_{1,\text{eff(y)}} = 0.1777, \ k_{2,\text{eff(y)}} = 0.0988 \ \text{and} \ k_{3,\text{eff(y)}} = 0.1777$$
 (64)

and,

$$k_{yy} = 0.1517 \frac{W}{m \, K} \tag{65}$$

In the *z*-direction:

$$k_{1,\text{eff}(z)} = 0.0988, k_{2,\text{eff}(z)} = 0.1777 \text{ and } k_{3,\text{eff}(z)} = 0.0988$$
 (66)

hence,

$$k_{zz} = 0.1256 \frac{W}{mK} \tag{67}$$

The above estimated value is close to the range specified in Srivaro *et al.* (2021). The estimated values for each case are listed in Table 2. This table demonstrates the accuracy of the derived equations in estimating thermal conductivity. The results closely aligned with experimental measurements for the CLT panels, underscoring the reliability of the generalized equations. Based on the results presented in Table 2 for both softwood and hardwood specimens, edge-gluing does not have a significant impact on the effective thermal conductivity of CLT panels (less than 2%) if the boards are tightly placed next to each other.

**Table 2.** Comparison of Predicted Thermal Conductivity  $(\frac{W}{mK})$  with Experimental Values (Refer to Fig. 4 for the x, y, and zCLT Directions)

| Softwood CLT                 |              |          |          |          |  |  |
|------------------------------|--------------|----------|----------|----------|--|--|
| Case 1 - Not Edge Glued CLT  |              |          |          |          |  |  |
|                              |              | $k_{xx}$ | $k_{yy}$ | $k_{zz}$ |  |  |
| Spruce (Picea orientalis L.) |              | 0.0661   | 0.1196   | 0.0661   |  |  |
| Polyurethane                 |              | _        | 0.513    | _        |  |  |
| Spruce CLT                   | Model        | 0.0667   | 0.1038   | 0.0862   |  |  |
|                              | Experimental | _        | 0.1032   | _        |  |  |
|                              | Error        |          | 0.58%    |          |  |  |
| Case 2 - Edge Glued CLT      |              |          |          |          |  |  |
| Spruce (Picea orientalis L.) |              | 0.0661   | 0.1196   | 0.0661   |  |  |
| Polyurethane                 |              | _        | 0.513    | _        |  |  |
|                              | Model        | 0.06846  | 0.1053   | 0.0877   |  |  |
| Spruce CLT                   | Experimental | _        | 0.1032   | _        |  |  |
| -                            | Error        |          | 2.03%    |          |  |  |
|                              |              |          |          |          |  |  |
|                              | Hardwood CLT |          |          |          |  |  |
| Case 1 - Not Edge Glued CLT  |              |          |          |          |  |  |
| Coconut Wood                 |              | 0.0987   | 0.1777   | 0.0987   |  |  |
| Melamine Urea-Formaldehyde   |              | -        | 0.1944   | _        |  |  |
|                              | Model        | 0.0991   | 0.1517   | 0.1255   |  |  |
| Coconut Wood CLT             | Experimental | -        | 0.153    | _        |  |  |
|                              | Error        | _        | 0.86%    | _        |  |  |
| Case 2 - Edge Glued CLT      |              |          |          |          |  |  |
| Coconut Wood                 |              | 0.0987   | 0.1777   | 0.0987   |  |  |
| Polyvinyl Acetate            |              | _        | 0.2      | _        |  |  |
| Melamine Urea-Formaldehyde   |              | _        | 0.1944   | -        |  |  |
|                              | Model        | 0.0992   | 0.1517   | 0.1256   |  |  |
| Coconut Wood CLT             | Experimental | _        | 0.153    | _        |  |  |
|                              | Error        | _        | 0.86%    | _        |  |  |

#### CONCLUSIONS

Investigating the effective thermal conductivity properties of wood becomes essential for understanding the coupling between mechanical and thermal properties, and the dimensional stability of large wood composite panels in three orthogonal directions.

This study introduced an analytical modeling approach based on the basic principles of micromechanics to study the orthotropic thermal conductivity of laminated wood composites. Some of the main findings are highlighted below.

- 1. Initially tailored for a three-layer cross-laminated timber (CLT) panel, the derived equations exhibited remarkable flexibility, easily adapting to accommodate CLT panels with more wood layers. This versatility ensures the equations maintain their predictive ability, making them highly practical for a wide range of CLT panel designs with a range of wood species and adhesive types.
- 2. An intriguing aspect of this study is the alignment between the Halpin-Tsai model and the series and parallel models used in the formation of the generalized equations. This alignment demonstrates the relevance of the derived equations in establishing a solid foundation for predicting not only the effective thermal conductivities of CLT panels but estimating their effective elastic moduli with various mixed species.
- 3. The proposed simplified model treats the resin as a continuous, isotropic solid. Imperfect glue lines or air gaps could be considered as alterative resin layers with modified properties; reduced values for imperfect glue lines or very low values representing the thermal conductivity of air may be assumed using the same approach. Voids within the resin-wood interface often exists and could be treated as a homogenized solid with a reduced or negligible thermal conductivity compared to resin.

The analytical-based micromechanical modeling approach presented here, along with its flexible generalized equations, provides valuable insights into thermal behavior of CLT panels. Results illustrated the high effectiveness of the derived equations in estimating thermal conductivities of various softwood and hardwood panels, closely matching experimental measurements, and highlighting the reliability and accuracy of the generalized equations.

## **ACKNOWLEDGMENTS**

The authors gratefully acknowledge the financial support of the University of Victoria and Natural Sciences and Engineering Research Council of Canada (NSERC). Additionally, financial support to the first author through MITACS Globalink Research Internship (GRI) program is acknowledged.

## **Data Availability Statement**

Data available on request from the authors.

# **Declaration of Conflicting Interests**

The authors are declared no potential conflicts of interest with respect to the research, authorship, and/or publication of this article.

## **REFERENCES CITED**

- Afshari, Z., and Malek, S. (2022). "Moisture transport in laminated wood and bamboo composites bonded with thin adhesive layers A numerical study," *Constr. Build. Mater.* 340(2022), article ID 127597. DOI: 10.1016/j.conbuildmat.2022.127597
- Akkaoui, A., Caré, S., and Vandamme, M. (2017). "Experimental and micromechanical analysis of the elastic properties of wood-aggregate concrete," *Constr. Build. Mater.* 134(44), 346-357. DOI: 10.1016/j.conbuildmat.2016.12.084
- Ashton, J., Halpin, J., and Petit, P. (1969). *Primer on Composite Materials' Analysis*, Technomic Publishing Co., Inc., Stamford, CT, USA.
- Aytin, A., Uygur, İ., Demirci, T., and Akgül, İ. (2022). "The effect of cryogenic treatment on some chemical, physical, and mechanical properties of Thermowood® Oriental spruce," *BioResources* 17(4), 6983–6996. DOI: 10.15376/biores.17.4.6983-6996
- Azemati, A. A., Khorasanizadeh, H., Hadavand, B. S., and Sheikhzadeh, G. A. (2018). "Experimental study on thermal conductivity of polyurethane resin filled with modified nanoparticles," *J. Comput. Appl. Res. Mech. Eng.* 8(1), 97-106. DOI: 10.22061/jcarme.2018.3063.1329
- Bučar, B., and Straže, A. (2007). "Determination of the thermal conductivity of wood by the hot plate method: The influence of morphological properties of fir wood (*Abies alba* Mill.) to the contact thermal resistance," *Holzforschung* 62(3), 362-367. DOI: 10.1515/hf.2008.021
- Chiniforush, A. A., Ataei, A., Valipour, H. R., Ngo, T. D., and Malek, S. (2022). "Dimensional stability and moisture-induced strains in spruce cross-laminated timber (CLT) under sorption/desorption isotherms," *Construction and Building Materials*, 356, article 129252. DOI: 10.1016/j.conbuildmat.2022.129252
- Claucherty, S., and Sakaue, H. (2018). "Phenol-formaldehyde resin for optical-chemical temperature sensing," *Sensors* 18(6), article 1756. DOI: 10.3390/s18061756
- Czajkowski, Ł., Olek, W., and Weres, J. (2020). "Effects of heat treatment on thermal properties of European beech wood," *Eur. J. Wood Wood Prod.* 78(3), 425-431. DOI: 10.1007/s00107-020-01525-w
- Díaz, A. R., Saavedra Flores, E. I., Yanez, S. J., Vasco, D. A., Pina, J. C., and Guzmán, C. F. (2019). "Multiscale modeling of the thermal conductivity of wood and its application to cross-laminated timber," *Int. J. Therm. Sci.* 144, 79-92. DOI: 10.1016/j.ijthermalsci.2019.05.016
- Eitelberger, J., and Hofstetter, K. (2011). "Prediction of transport properties of wood below the fiber saturation point A multiscale homogenization approach and its experimental validation. Part II: Steady state moisture diffusion coefficient," *Compos. Sci. Technol.* 71(2), 145-151. DOI: 10.1016/j.compscitech.2010.11.006
- Griffiths, E., and Kaye, G. W. C. (1923). "The measurement of thermal conductivity," *P. Roy. Soc. A- Math. Phy.* 104(724), 71-98. DOI: 10.1098/rspa.1923.0095
- Kol, H. Ş., and Altun, S. (2009). "Effect of some chemicals on thermal conductivity of impregnated laminated veneer lumbers bonded with poly(vinyl acetate) and melamine–formaldehyde adhesives," *Dry. Technol.* 27(9), 1010-1016. DOI: 10.1080/07373930902905092
- Kühlmann, G. (1962). "Untersuchung der thermischen Eigenschaften von Holz und Spanplatten in Abhängigkeit von Feuchtigkeit und Temperatur im hygroskopischen Bereich [Investigation of the thermal properties of wood and chipboard depending on

- moisture and temperature in the hygroscopic range]," *Holz. Roh. Werkst.* 20(7), 259-270. DOI: 10.1007/bf02604682
- Li, T., Song, J., Zhao, X., Yang, Z., Pastel, G., Xu, S., Jia, C., Dai, J., Chen, C., Gong, A., *et al.* (2018). "Anisotropic, lightweight, strong, and super thermally insulating nanowood with naturally aligned nanocellulose," *Science Advances* 4(3), article ID aar3724. DOI: 10.1126/sciadv.aar3724
- MacLean, J. D. (1941). "Thermal conductivity of wood," *Heat-Piping-Air Cond.* 13, 380-391.
- Malek, S., and Gibson, L. (2017). "Multi-scale modelling of elastic properties of balsa," *Int. J. Solids Struct.* 113-114, 118-131. DOI: 10.1016/j.ijsolstr.2017.01.037
- Malekmohammadi, S., Zobeiry, N., Gereke, T., Tressou, B., and Vaziri, R. (2015). "A comprehensive multi-scale analytical modelling framework for predicting the mechanical properties of strand-based composites," *Wood Sci. Technol.* 49(1), 59-81. DOI: 10.1007/s00226-014-0682-8
- Malek, S., Nadot-Martin, C., Tressou, B., Dai, C., and Vaziri, R. (2019). "Micromechanical modeling of effective orthotropic elastic and viscoelastic properties of parallel strand lumber using the morphological approach," *J. Eng. Mech.* 145(9), article 4019066. DOI: 10.1061/(ASCE)EM.1943-7889.0001
- Narayanamurti, D., and Ranganathan, V. (1941). "The thermal conductivity of Indian timbers," *P. Indian Acad. Sci. A* 13(4), 300-315. DOI: 10.1007/bf03049008
- Niemz, P., and Sonderegger, W. (2017). "Geschichte der Physik des Holzes [History of the physics of wood]," in: *Holzphysik*, Carl Hanser Verlag GmbH & Co. KG, Munich, Germany, pp. 27-35. DOI: 10.3139/9783446445468.002
- Öztürk, H., Yücesoy, D., and Çolak, S. (2020). "Thermal conductivity of cross laminated timber (CLT) with a 45° alternating layer configuration," *Wood Industry & Engineering* 2(1), 13-16.
- Qiao, Z., and Mao, J. (2017). "Multifunctional poly (melamine-urea-formaldehyde)/ graphene microcapsules with low infrared emissivity and high thermal conductivity," *Mater. Sci. Eng. B- Adv.* 226, 86-93. DOI: 10.1016/j.mseb.2017.08.016
- Ratcliffe, E. H. (1964). "A review of thermal conductivity data," Wood 29(8), 46-49.
- Ross, R. J. (2010). Wood Handbook: Wood as an Engineering Material (FPL-GTR-190), U.S. Department of Agriculture, Forest Products Laboratory, Forest Service, Madison, WI, USA.
- Saavedra Flores, E. I., Dayyani, I., Ajaj, R., Castro-Triguero, R., DiazDela, O. F., Das, R., and Gonz'alez Soto, P. (2015). "Analysis of cross-laminated timber by computational homogenization and experimental validation," *Compos. Struct.* 121, 386-394. DOI: 10.1016/j.compstruct.2014.11.042
- Saripally, A. (2015). A Micromechanical Approach to Evaluate the Effective Thermal Properties of Unidirectional Composites, Master's Thesis, Birla Institute of Technology and Science, Rajasthan, India. DOI: 10.13140/RG.2.1.4842.8966.
- Sonderegger, W., Hering, S., and Niemz, P. (2011). "Thermal behaviour of Norway spruce and European beech in and between the principal anatomical directions," *Holzforschung* 65(3), 369-375. DOI: 10.1515/hf.2011.036
- Srivaro, S., Pásztory, Z., Le Duong, H. A., Lim, H., Jantawee, S., and Tomad, J. (2021). "Physical, mechanical and thermal properties of cross laminated timber made with coconut wood," *Eur. J. Wood Wood Prod.* 79(6), 1519-1529. DOI: 10.1007/s00107-021-01741-y

- Steinhagen, H. P. (1977). Thermal Conductive Properties of Wood, Green and Dry, From -40 °C to +100 °C: A Literature Review (GTR-FPL-9), U.S. Department of Agriculture, Forest Service, Forest Products Laboratory, Madison, WI, USA.
- Taoukil, D., El Bouardi, A., Sick, F., Mimet, A., Ezbakhe, H., and Ajzoul, T. (2013). "Moisture content influence on the thermal conductivity and diffusivity of wood concrete composite," *Constr. Build. Mater.* 48, 104-115. DOI: 10.1016/j.conbuildmat.2013.06.067
- Temizer, İ., and Wriggers, P. (2010). "A micromechanically motivated higher-order continuum formulation of linear thermal conduction," *ZAMM Z. Angew. Math. Me.* 90(10–11), 768-782. DOI: 10.1002/zamm.201000009
- Vay, O., Busquets-Ferrer, M., Emsenhuber, G., Huber, C., Gindl-Altmutter, W., and Hansmann, C. (2021). "Thermal conductivity of untreated and chemically treated poplar bark and wood," *Holzforschung* 75(12), 1125-1135. DOI: 10.1515/hf-2020-0268
- Vay, O., Obersriebnig, M., Müller, U., Konnerth, J., and Gindl-Altmutter, W. (2013). "Studying thermal conductivity of wood at cell wall level by scanning thermal microscopy (SThM)," *Holzforschungs* 67(2), 155-159. DOI: 10.1515/hf-2012-0052
- Wangaard, F. F. (1940). "Transverse heat conductivity of wood," *Heat-Piping-Air Cond*. 12, 459-464.

Article submitted: February 12, 2024; Peer review completed: March 30, 2024; Revised version received and accepted: January 3, 2025; Published: January 22, 2025. DOI: 10.15376/biores.20.1.2150-2170